Journal of Polymer Research (2023) 30:199
https://doi.org/10.1007/s10965-023-03572-2

ORIGINAL PAPER

# Bio-inspired antibacterial polymer coatings with included silver nanoparticles and porphyrin-based photosensitizer

**Rayna Bryaskova[1] · Nikoleta Philipova[1] · Nikolai Georgiev[2] · Damyan Ganchev[3] · Ivo Lalov[4] · Christoph Detrembleur[5]**

Received: 8 March 2023 / Accepted: 20 April 2023


**Abstract**
In this work, we have prepared novel bio-inspired photoactive antibacterial polymer coatings on stainless steel (SS), which possess good mechanical and antibacterial properties. The formation of the photoactive antibacterial polymer coatings consists of the sequential deposition of three components on SS substrate (1) a catechol-based cationic glue P(mDOPA)-*co*-P(DMAEMA$^+$) used as a universal primer, which facilitates the strong anchoring to SS; (2) a silver loaded (Pox(mDOPA)-Ag$^0$/PAH) nanogel decorated with *o*-quinones applied to enhance the antibacterial properties of the coating and to permit the covalent grafting of the photosensitizer, and (3) an ethylene diamine derivative of protoporphyrin IX (PPIX-ED). Porphyrins are widely recognized for their antibacterial activity by producing reactive oxygen species when exposed to visible light. To estimate the deposition of the components on the SS substrate, SEM-EDX elemental mapping analysis was applied. Scratch test, nanoindentation, and accelerated property mapping (XPM) analysis were used to assess the mechanical properties of the coatings. The established antibacterial activity of the prepared photoactive polymer coatings on SS against Gram-positive *B. subtilis* and Gram-negative *E. coli* strains demonstrates their potential applications in medical and biomedical fields.

**Keywords** Coatings · Adhesion · Nanomaterials · Silver nanoparticles · Porphyrins

## Introduction

Due to the increasing number of infectious diseases caused by pathogenic or conditionally pathogenic microorganisms, many research groups are directing their activities to develop alternative and more effective products that possess "permanent" antibacterial activity without the risk of generating resistance to them. This is of particular importance for hospital facilities, where the presence of nosocomial infections caused by various pathogens is a serious problem and is one of the main reasons for increased patient morbidity and mortality and has a large financial impact on hospital resources [1]. Therefore, the development of appropriate products for surface disinfection is of great importance to control and prevent the spread of these infections. In recent years, light-activated antimicrobial coatings containing organic and/or inorganic photosensitizers are considered as promising products that possess continuous antibacterial activity against bacteria, viruses, and fungi [2]. This is due to the property of photosensitizers to absorb light energy with an appropriate wavelength that transmits it to the surrounding molecules (mainly to oxygen), thus forming reactive oxygen species (ROS) (radicals and singlet oxygen). These highly reactive species are responsible for the destruction of the attacked cells [3, 4].

The preparation of light-activated antibacterial surfaces on the base of phenothiazine dyes, such as toluidine blue or methylene blue incorporated into a polymer matrix by applying swell-encapsulation-shrink methodology was reported [5, 6]. However, these materials do not generate a large

✉ Rayna Bryaskova
rbryaskova@uctm.edu

1 Department of Polymer Engineering, University of Chemical Technology and Metallurgy, Sofia, Bulgaria

2 Department of Organic Synthesis, University of Chemical Technology and Metallurgy, Sofia, Bulgaria

3 Department of Machine Elements and Non-Metal Constructions, Technical University, Sofia, Bulgaria

4 Department of Biotechnology, University of Chemical Technology and Metallurgy, Sofia, Bulgaria

5 CESAM Research Unit, Chemistry Department, Center for Education and Research on Macromolecules (CERM), University of Liege, Liège, Belgium

Published online: 11 May 2023

number of reactive oxygen species on irradiation, and gold nanoparticles were used to enhance their properties [7–10]. Moreover, there is a risk of leaching the photosensitizer from the polymer matrix, which can reflect on biocompatibility and patient safety. To avoid this, in another case, the surface attachment of boro-dipyrromethane (BODIPY) to the surface of a sample polymer, poly(dimethylsiloxane) (PDMS), was reported and their antibacterial activity against *Staphylococcus aureus* (*S. aureus*) and *Escherichia coli* (*E. coli*) was demonstrated [11].

In another approach, light-activated antimicrobial coatings were obtained by electrodeposition technique of metal-containing phthalocyanines on indium tin oxide/borosilicate glass or glass surfaces, and their activity against gram-positive *S. aureus* under visible-light illumination was reported [12, 13]. The main limitation of the preparation of such types of coatings in large-scale production is the ease and accessibility of a deposition procedure.

Recently, we reported on the preparation of mussels-inspired photoactivate antibacterial coatings on stainless steel (SS) with grafted photosensitizer of the 9-aminoacridine-3 type. The photoactive antibacterial coatings were based on a quinone-decorated nanogel deposited on a surface precoated by bio-inspired glue, a cationic polyelectrolyte bearing pendent catechols, and a grafted photosensitizer of the aminoacridine [14]. The coatings demonstrated good surface and mechanical properties with pronounced antibacterial activity against G. negative *E. coli*. The use of a cationic polyelectrolyte bearing pendent catechols [15], as well as a quinone-decorated nanogel [17], was demonstrated as a power tool responsible for the good adhesion to the subtract due to the presence of adhesive 3,4-dihydroxy-L-phenylalanine (DOPA) repeating units in the polymer chains [15–19].

Based on this, here, we report on the preparation of bio-inspired photoactive antimicrobial polymer coatings based on an *o*-quinone functionalized nanogel, loaded with silver nanoparticles Pox(mDOPA)-$Ag^0$/PAH, and a photosensitizer based on an ethylene diamine derivative of protoporphyrin IX (PPIX-ED). Among the photosensitizers, protoporphyrin IX (PPIX) attracts special attention, since, in addition to its high photoactivity, is widely recognized for its antibacterial activity by producing reactive oxygen species when exposed to visible light, and is a native compound present in humans as a precursor in heme synthesis [20–22]. It is well known, that silver nanoparticles possess high bactericidal activity against Gram-negative and Gram-positive bacteria due to a complex mechanism of action, and it is more difficult for bacteria to develop a resistance to silver in comparison to conventional used means [23]. Moreover, the use of silver nanoparticles in addition to enhance their antibacterial activity can protect the porphyrin against photobleaching and for the conservation of energy [24, 25].

## Materials and methods

Protoporphyrin IX (PPIX) (Sigma-Aldrich), N-Hydroxysuccinimide (NHS), and 1-(3-Dimethylaminopropyl)-3-ethyl carbodiimide hydrochloride, 98+% (EDC) (Alfa Aesar) and Polyallylamine hydrochloride (PAH) (Sigma-Aldrich) were used without further purification. Stainless steel (SS) 316 was used as a substrate. Poly(N-methacryloyl 3,4-dihydroxy-L-phenylalanine methyl ester)-b-poly(2-methacryloxyethyltrimethylammonium chloride) (P(mDOPA)-*co*-P($DMAEMA^+$) copolymer [15], Poly(N-methacryloyl 3,4-dihydroxy-L-phenylalanine methyl ester) (P(mDOPA)) [16], and a silver loaded (Pox(mDOPA)-$Ag^0$/PAH) cross-linked nanogel [17] were prepared as reported in the mentioned publications [15–17].

### Synthesis of ethylene diamine derivative of protoporphyrin IX (PPIX-ED)

Ethylene diamine derivative of protoporphyrin IX (PPIX-ED) was prepared according to the procedure reported in [22]. In brief, protoporphyrin IX (200 mg, 0.355 mmol) was dissolved in 20 mL DMF (pre-purged with $N_2$) at room temperature. Ethylene diamine (40 mg, 0.666 mmol), NHS (40 mg, 0.348 mmol), and EDC (190 mg, 0.991 mmol) were added sequentially to the resulting solution under stirring at room temperature. After 30 min a fine precipitate was formed. The resulting mixture was then allowed to stir for 24 h at room temperature.

### Synthesis of silver loaded (pox(mDOPA-$Ag^0$)/PAH) cross-linked nanogel

The synthesis of silver loaded (Pox(mDOPA)-$Ag^0$/PAH) cross-linked nanogels was performed according to [17]. In brief, 10 mg of P(mDOPA) was dissolved in 9 mL of deionized $H_2O$. The resulting solution was stirred at room temperature for 2 h. Then an aqueous solution of $AgNO_3$ (1 ml, $5.8.10^{-2}$ M) was added dropwise under vigorous stirring. A milky white suspension was obtained which was allowed to stir at room temperature for 20 h. Then, 3 mL of an aqueous solution of PAH (1 g $L^{-1}$) at pH > 9 was added to the solution and stirred for 2 h at room temperature.

### Preparation of the photoactive polymer coatings on SS substrate

Stainless steel samples with different sizes were cut out from the as-received 1 mm thick SS, 1.0 cm x 1.0 cm. They were cleaned and degreased by washing for 2 min with ethanol and acetone respectively and dried with nitrogen. The coatings were conducted at room temperature. The substrate

was first dipped in an aqueous solution of P(DOPA)-*co*-P(DMAEMA$^+$) (2 g L$^{-1}$, pH 7) for 15 min, then rinsed in deionized water for 5 min, followed by dipping into an aqueous solution of Pox(mDOPA)-Ag$^0$/PAH nanogel (1 g L$^{-1}$) for 15 min and rinsed with deionized water for 5 min. The final deposition was an ethanol solution of amino modified Protoporphyrin IX (1 g L$^{-1}$, pH 10), wherein the substrate was dipped for 15 min followed by rinsing with deionized water for 5 min.

### Characterizations

ATR FT-IR spectra were recorded using Agilent Cary 600 equipment. The proton nuclear magnetic resonance ($^1$H NMR) spectroscopy spectra were recorded on Brucker Advance III HD 400 using DMSO-d6 as a solvent. Transmission electron microscopy (TEM) observations were carried out with an HR STEM JEOL JEM 2100 instrument. Samples were prepared by deposition of a droplet of the aqueous silver loaded nanogels solution onto a carbon coated copper TEM grid, which was allowed to evaporate for 2 h. SEM-EDX spectra were recorded on SEM Lyra, Tescan with Quantax EDS detector – Bruker. Dynamic light scattering (DLS) measurements were performed using Brookhaven instruments (NanoBrook 90Plus) with ZetaPlus Particle Sizing Software Version 5.23. Scattering data are collected at 70 individual measurements at a constant scattering angle and averaged for each sample. The inhibition zones of the tested samples were measured using Image-Pro Plus software.

#### Scratch test with spherical-conical stylus

Scratch testing was performed using UMT (Bruker) scratch test module with a diamond spherical-conical stylus with tip radius (DSH-025, R = 2.5 µm) over a scratch distance of 5 mm with a scratch speed of 0.083 mm/s with gradually increased load from 5 to 50 mN. All scratches were carried out five times in the same direction. A progressive loading scratch test mode was performed, where the load on the indenter increases linearly as the indenter moves across the test surface at a constant speed, and failure was observed. An x-axis slider moves the diamond stylus across the test specimen to produce the scratch. The UMT equipment allows monitoring during the test of the actual normal force, scratching force, and coefficient of friction. The scratch line was observed by SEM (Tabletop Hirox SH-4000 M).

#### Nanoindentation measurement

Nanomechanical analyses were performed using Universal Nanomechanical Tester (UNMT, Bruker), equipped with Nanoindenter & Atomic Force Microscopy (AFM, Ambios Technology). For each specimen, 48 nanoindentations were made with force applied to 50 mN. The 70 nm diamond tip Berkovich indenter was used to perform the tests and specialized software to calculate the hardness and the modulus of elasticity of the specimens using the Oliver Pharr method [26]. All nanoindentation tests were performed at a constant temperature of 20 °C. Accelerated property mappings (XPM), have been performed on Hysitron TI 980 instrument (Bruker, Billerica, MA, USA).

### Photobactericidal activity

The photobactericidal activity of Pox(mDOPA)-Ag$^0$/PAH and PPIX-ED compounds and P(mDOPA)-*co*-P(DMAEMA$^+$)/Pox(mDOPA)-Ag$^0$/PAH and P(mDOPA)-*co*-P(DMAEMA$^+$)/Pox(mDOPA)-Ag$^0$/PAH/PPIX-ED coatings against Gram-negative bacteria *E. coli* and Gram-positive bacteria *B. subtilis* was assessed by disk-diffusion method (DDM) modified by using a light source, necessary to ensure the photodynamic activity. For Pox(mDOPA)-Ag$^0$/PAH and PPIX-ED compounds, the test was performed by using disks from chromatographic paper (d = 6 mm), which were impregnated with 5 µL of the solutions, and for the coatings, the test was performed using SS substrate (1 × 1 cm). In this procedure, agar plates were inoculated with 0.2 mL standardized inoculum (10$^7$ cells. mL$^{-1}$) of the test microorganism. Then samples were sterilized by UV irradiation and placed on the agar surface. The Petri dishes were illuminated using a 300 W spotlight (wavelength from 380 to 750 nm) and incubated under suitable conditions (30°C for *B. subtilis* and 37°C for *E. coli*) for 24 h. Then the diameters of inhibition growth zones were measured. The antibacterial activity of neat SS substrate as a control sample was also tested under the same conditions.

## Results and discussion

### Preparation of the photoactive antibacterial polymer coating on stainless steel

The photoactive antibacterial polymer coatings (Scheme 1) were prepared by the sequential deposition of three solutions consisting of: (1) bio-inspired cationic polymer bearing pendent catechols; (2) silver-loaded Pox(mDOPA)-Ag$^0$/PAH nanogel decorated with *o*-quinone groups and (3) amino-modified protoporphyrin IX as a photosensitizer (PPIX-ED).

The first layer, a catechol-based cationic copolymer P(mDOPA)-*co*-P(DMAEMA$^+$) (2 g L$^{-1}$) solution was used to ensure the strong anchoring of the final coating to the substrate of SS as reported in the literature [15–18]. As a second layer, silver loaded *o*-quinones decorated nanogel based on Pox(mDOPA)/PAH were applied, which possesses

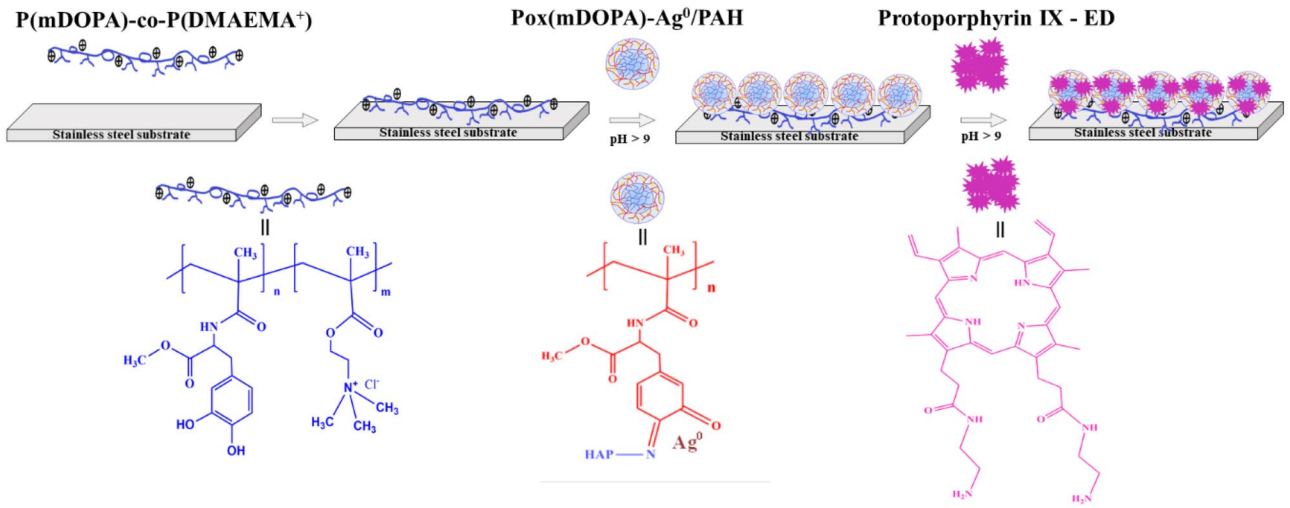


**Scheme 1** Strategy for preparing of bio-inspired photoactive polymer coatings on the base of silver loaded Pox(mDOPA)-$Ag^0$/PAH nanogels and amino-modified PPIX-ED.

a dual function: (i) to permit the covalent grafting of the amino-bearing photosensitizer by reaction of its amine groups with the quinone groups present in the nanogels and (ii) to enhance the antibacterial properties of the coatings. For this purpose, Pox(mDOPA)-$Ag^0$/PAH nanogels were prepared by the addition of a PAH solution (1 g $L^{-1}$) to the silver loaded Pox(mDOPA) aqueous solution (Scheme 2) as reported by Faure et al. [17], resulting in the appearance of a yellow-brown suspension.

To prove the successful formation of silver nanoparticles (AgNPs) loaded into the crosslinked nanogels based on Pox(mDOPA)/PAH, the antibacterial nanogel was characterized by TEM and DLS analysis (Fig. 1). The TEM images clearly demonstrated the formation of silver loaded Pox(mDOPA)/PAH nanogel particles with a diameter having an average size of 15.6 ± 4.6 nm (Fig. 1a), in line with previous data [17]. The performed selected area electron diffraction (SAED) pattern showed characteristic diffraction rings corresponding to (111), (200), (220), and (311) reflections of the fcc (face-centered cubic) structure of silver and confirmed the crystalline nature of the silver nanoparticles (Fig. 1b) [27]. DLS analysis showed the formation of silver loaded nanogel particles with an average hydrodynamic diameter (Dh) of 110 ± 10 nm, at an index of polydispersity (PDI) of 0.2 (Fig. 1c). The different diameter observed by DLS and TEM of Pox(mDOPA)-$Ag^0$/PAH nanogels is a result of the shrinkage of the nanoparticles in their dried state for TEM observation.

The last layer was formed by depositing of an ethylene diamine derivative of protoporphyrin IX (PPIX-ED) (1 g $L^{-1}$). The chemical modification of Protoporphyrin IX (Scheme 3) was necessary to ensure the presence of amino groups which were important for the covalent grafting to the second Pox(mDOPA)-$Ag^0$/PAH layer by the quinone groups

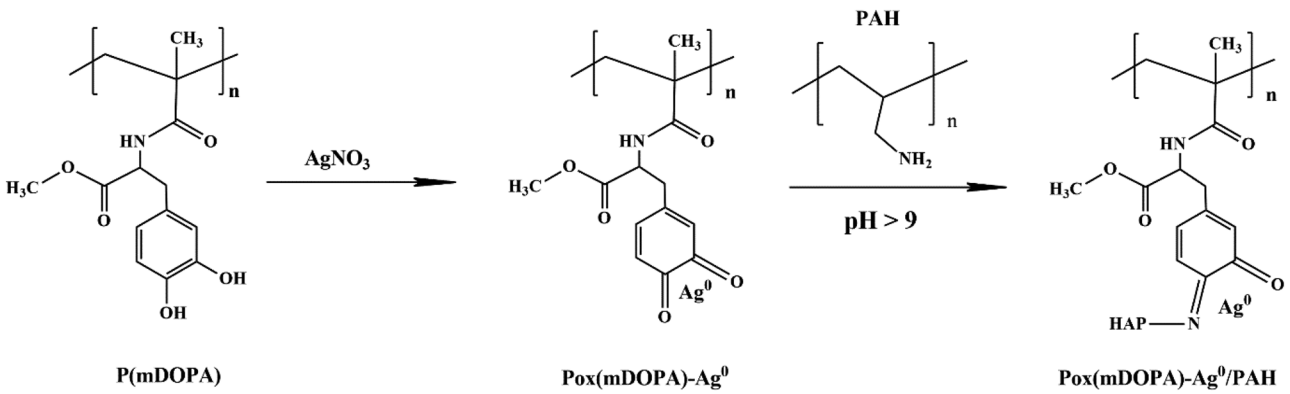


**Scheme 2** Strategy for preparation of silver loaded Pox(mDOPA)/PAH nanogels

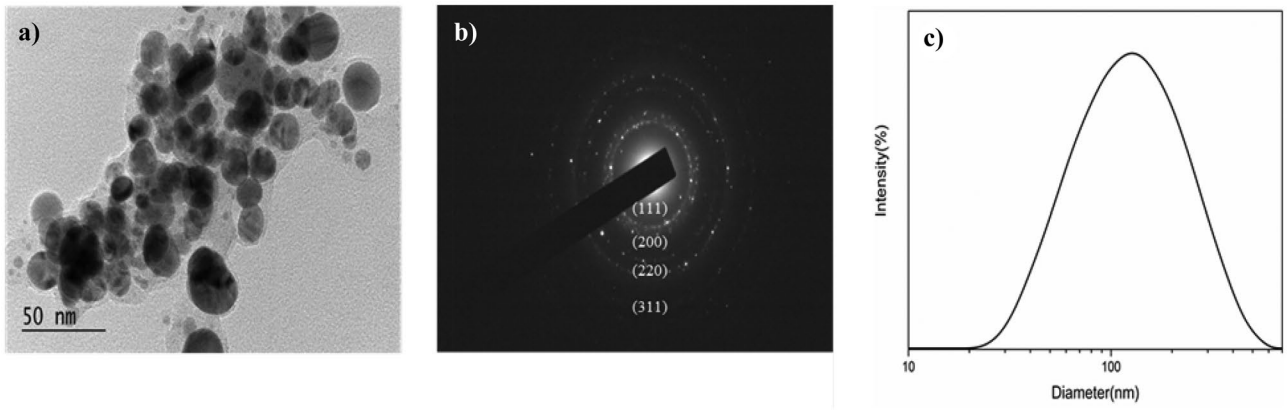


**Fig. 1** **a** TEM of silver loaded Pox(mDOPA)/PAH nanogels, **b** SAED of silver loaded Pox(mDOPA)/PAH nanogels and **c** DLS analysis of silver loaded Pox(mDOPA)/PAH nanogels

present in the nanogels through the well-known amine/quinone reactions [17]. The amino modified PPIX was synthesized in a one-step procedure by using an excess of ethylene diamine in the presence of EDC and NHS, which lead to the formation of the final product.

The performed ATR-FTIR and $^{1}$H NMR analyses (Fig. 2a, b) confirm the modification of PPIX by the presence of all characteristic peaks at 3300 $cm^{-1}$ for N–H stretching vibration; 2911 $cm^{-1}$ for asymmetric stretching vibration of $–CH_2–$; 2855 $cm^{-1}$ for symmetric stretching vibration of $–CH_2–$; 1628 $cm^{-1}$ for C = O stretching vibration of –CONH– (Amide I band) and at 1533 for C = O stretching vibration of –CONH– (Amide II band) (Fig. 2a). Furthermore, the $^{1}$H NMR clearly showed that the both carboxylic groups were modified with ethylenediamine. As can be seen from the $^{1}$H NMR spectrum of PPIX-ED, the resonance at 10.25 ppm corresponding to = CH– protons in porphyrine scaffold and resonance at 5.96 ppm attributed to the amide protons were in ratio 4:2, which revealed that two ethylenediamine units were bonded to a single porphyrine core (Fig. 2b).

## Surface and mechanical properties of the antibacterial polymer coatings

The surface and mechanical properties of thus obtained photoactive coatings were estimated by various techniques such as Energy Dispersive X-Ray Analysis with SEM (EDX-SEM), scratch test, nanoindentation, and accelerated property mapping (XPM).

### Energy dispersive x-ray analysis with SEM

The types and the distribution of the elements at the surface and near the surface of the coatings were estimated by providing an overall mapping of the samples using

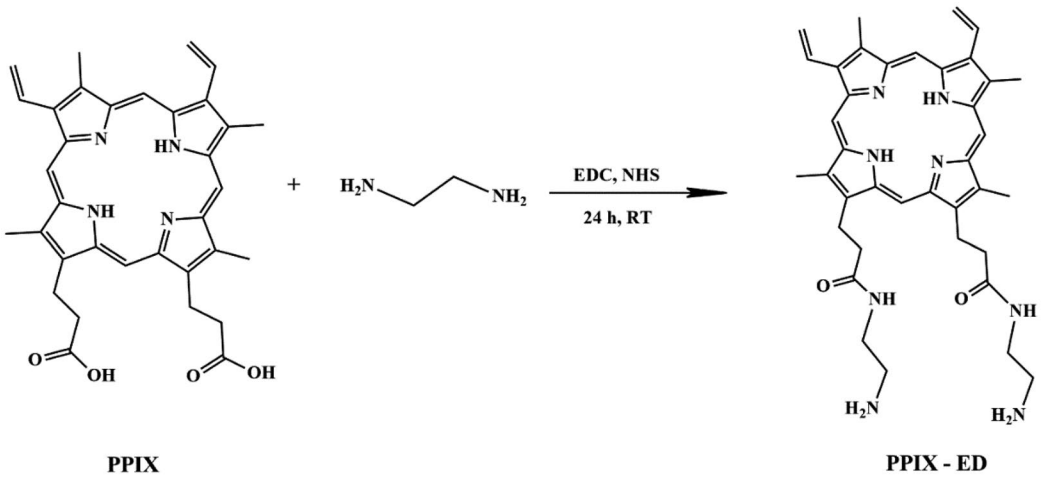


PPIX PPIX - ED

**Scheme 3** Synthesis of an ethylene diamine derivative of protoporphyrin IX

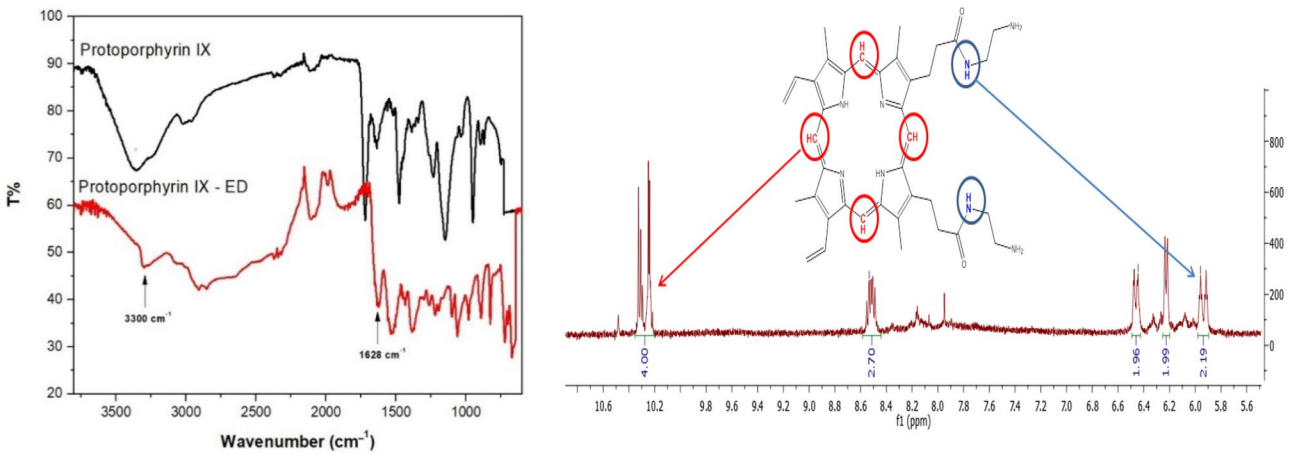


**Fig. 2** **a** ATR-FTIR of protoporphyrin IX and ethylene diamine derivative of protoporphyrin IX and **b** $^{1}$HNMR spectrum of the amino functionalized protoporphyrin IX

EDX-SEM analysis. Initially, P(mDOPA)-*co*-P(DMAEMA$^{+}$)/Pox(mDOPA)-Ag$^{0}$/PAH coatings on SS were characterized by EDX-SEM analysis to demonstrate the deposition of the silver-loaded nanogel and the presence of silver nanoparticles on the substrate. The elemental mapping indicated the uniform distribution of silver (Ag) as well as the presence of carbon (C) and nitrogen (N) on the SS substrate, which derived from the Pox(mDOPA)/PAH nanogel (Fig. 3a). The EDX elemental signal maps of the coating after deposition of the last photoactive PPIX-ED layer also demonstrated the existence of carbon (C), oxygen (O), and nitrogen (N). However, the presence of silver was not so pronounced. Moreover, some aggregates on the base of the synthesized PPIX-ED on the substrate were observed, where higher carbon contents of 64 at% were detected in comparison to other areas of the substrate where the carbon content was 57 at% (Fig. 3b).

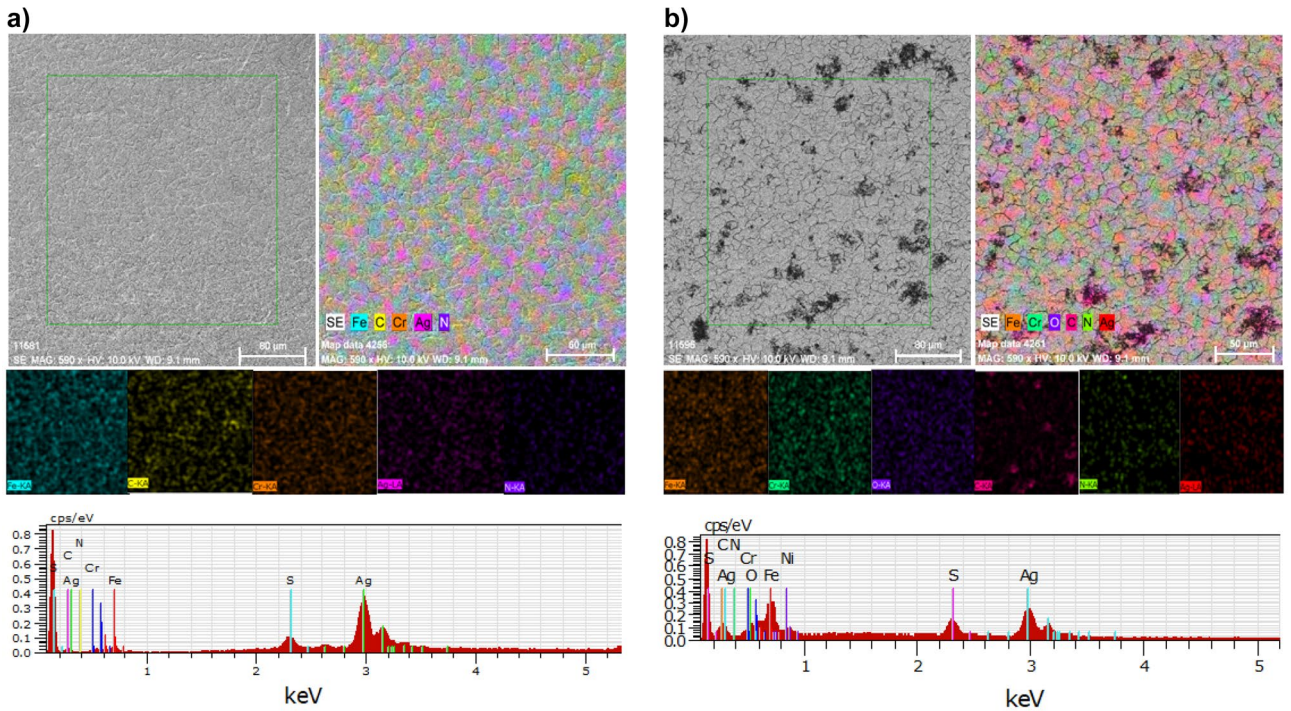


**Fig. 3** SEM-EDX mapping and elemental analysis in a point of **a** P(mDOPA)-*co*-P(DMAEMA$^{+}$)/Pox(mDOPA)-Ag$^{0}$/PAH coating on SS substrate and **b** P(mDOPA)-*co*-P(DMAEMA$^{+}$)/Pox(mDOPA)-Ag$^{0}$/PAH/PPIX-ED coating on SS substrate

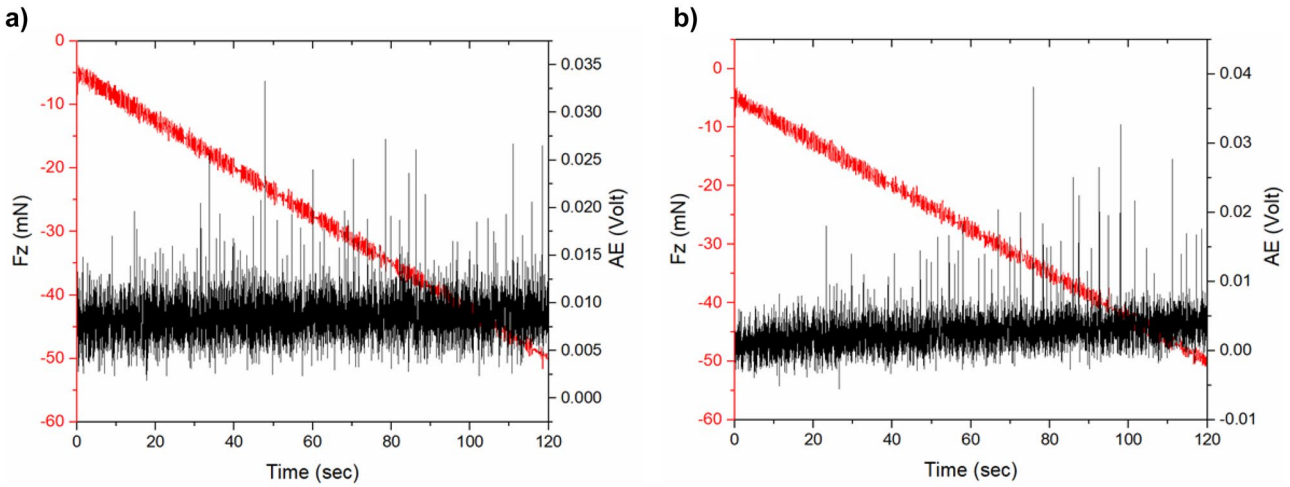


**Fig. 4** Scratch test on SS substrate of **a** P(mDOPA)-*co*-P(DMAEMA$^+$)/Pox(mDOPA)-Ag$^0$/PAH and **b** P(mDOPA)-*co*-P(DMAEMA$^+$)/Pox(mDOPA)-Ag$^0$/PAH/PPIX-ED; Fz – Normal force (mN), AE - acoustic emission (volt)

## Nanomechanical properties of the antibacterial polymer coatings on SS

**Scratch testing** Coatings are widely used in a variety of applications and whether they adhere sufficiently to the substrate is of great importance. In many cases, the adhesion of the coating to the substrate is a limiting factor for its use in certain applications. The scratch test was developed as a quick and simple method to test coating adhesion and consists of pressing a hard diamond or metal spherical-tipped indenter with a typical radius of 200 µm onto the surface of the coating, using either a constant or an increasing load, whilst moving the sample at a constant speed [28]. Scratching of the surface resulted in an increase in elastic and plastic deformation until extensive spalling of the coating from the substrate occurred at a critical load, which was generally determined using optical microscopy, acoustic emission, or friction force measurements. In the present study, the scratch test was performed on the SS substrate coated with P(mDOPA)-*co*-P(DMAEMA$^+$)/Pox(mDOPA)-Ag$^0$/PAH and P(mDOPA)-*co*-P(DMAEMA$^+$)/Pox(mDOPA)-Ag$^0$/PAH/PPIX-ED applying gradually increased load from 5 to 50 mN. Figure 4 shows the typical average load range at which the coating failed during scratch testing as the scratching process was accompanied by the emission of acoustic signals. For the P(mDOPA)-*co*-P(DMAEMA$^+$)/Pox(mDOPA)-Ag$^0$/PAH, the coating adhered at load until 20 mN, with a coefficient of friction (COF) of 0.53. For the P(mDOPA)-*co*-P(DMAEMA$^+$)/Pox(mDOPA)-Ag$^0$/PAH/PPIX-ED coating, the increase in the acoustic signal was detected at an even higher load of 30 mN with a coefficient of friction (COF) of 0.5. The coefficient of friction (COF) slightly decreased after the deposition of the last PPIX-ED layer, which was indicative of higher scratch resistance.

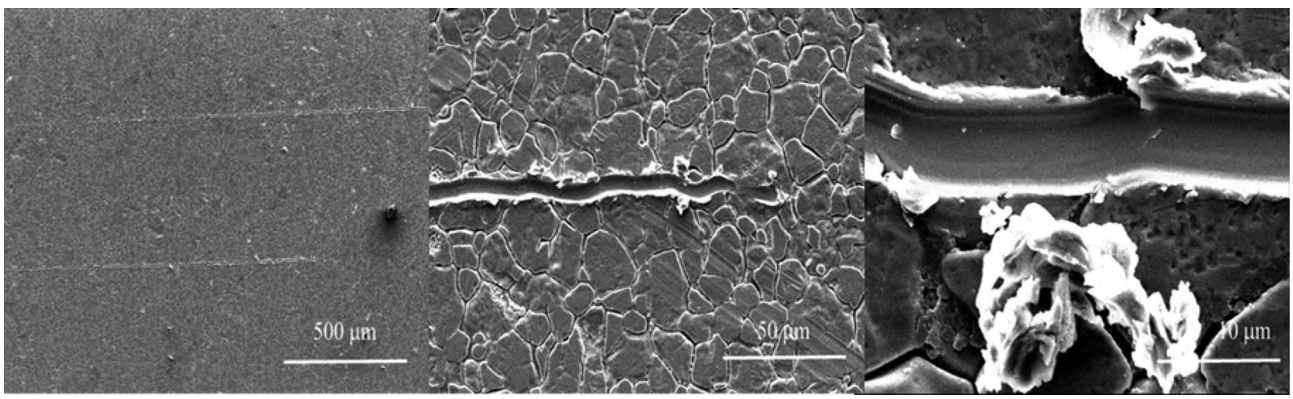


**Fig. 5** SEM images at different magnifications of the scratch track of P(mDOPA)-*co*-P(DMAEMA$^+$)/Pox(mDOPA)-Ag$^0$/PAH/PPIX-ED under loading from 5 to 50 mN

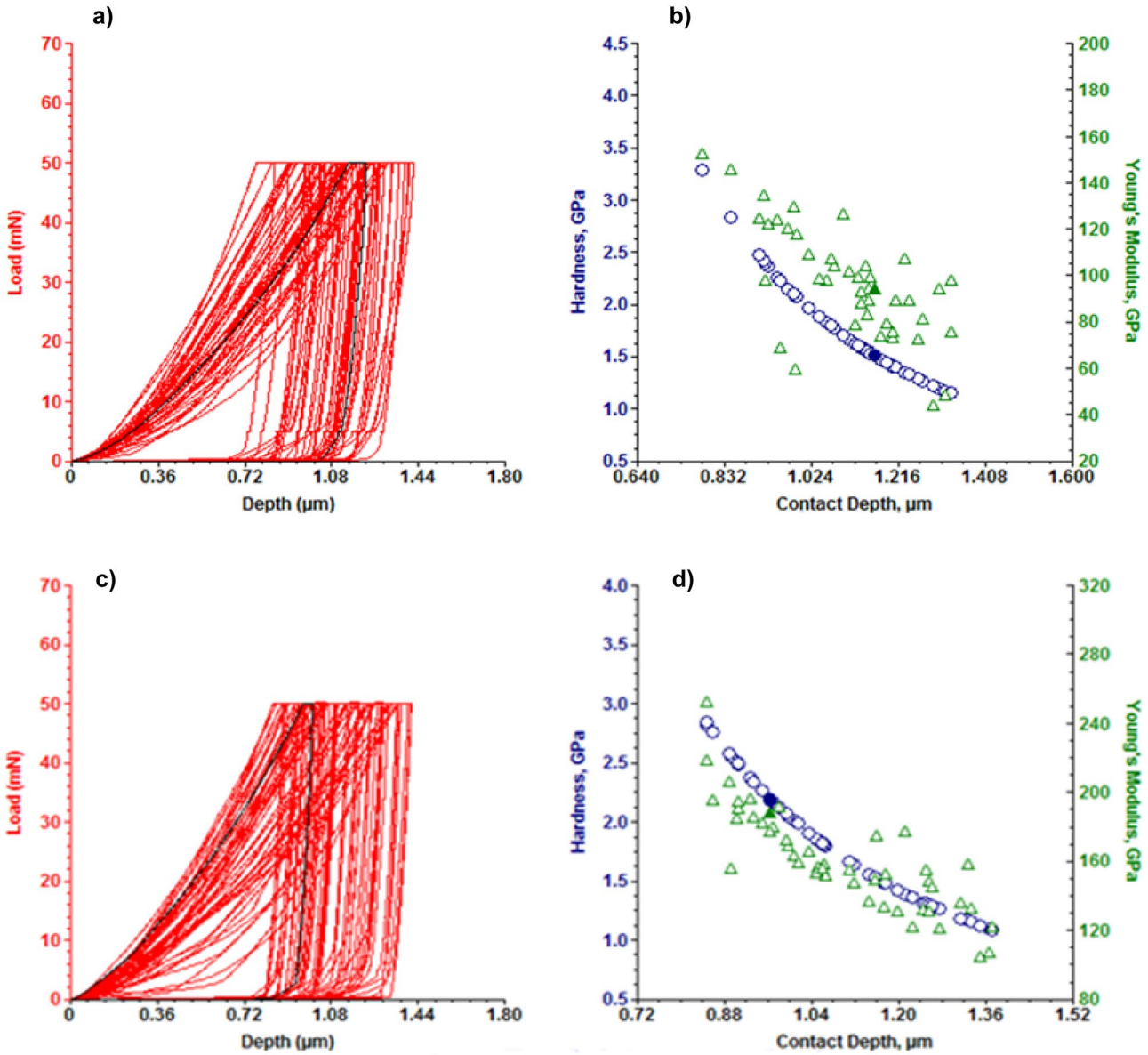


**Fig. 6** Nanoindentation curve, hardness (H) and elastic modulus (E) of: **a–b** P(mDOPA)-*co*-P(DMAEMA$^+$)/Pox(mDOPA)-Ag$^0$/PAH and **c–d** P(mDOPA)-*co*-P(DMAEMA$^+$)/Pox(mDOPA)-Ag$^0$/PAH/PPIX-ED

SEM images demonstrated a linear increasing scratch track on the coatings without cracking or delamination during the scratch test, and only a small amount of debris from the scratching was observed (Fig. 5). The obtained results of the scratch test demonstrated again good scratch resistance.

**Nanoindentation measurement of photoactivate polymer coatings** Nanoindentation is introduced as a method for determining the modulus and hardness of materials by studying nanomechanical response as a function of penetration depth [29]. In this method, the displacement (h) of materials under specifically applied loads (P) is investigated to produce load– displacement (P–h) curves. Anomalies in these curves relate to mechanical phenomena such as the onset of dislocations, cracks, and even crystalline phase transformations [29].

Therefore, it was interesting to study the nanomechanical properties of the obtained photoactive antibacterial coatings. For this purpose, the SS substrates coated with P(mDOPA)-*co*-P(DMAEMA$^+$)/Pox(mDOPA)-Ag$^0$/PAH and P(mDOPA)-*co*-P(DMAEMA$^+$)/Pox(mDOPA)-Ag$^0$/PAH/PPIX-ED were subjected to nanoindentation measurements (Fig. 6a-d).

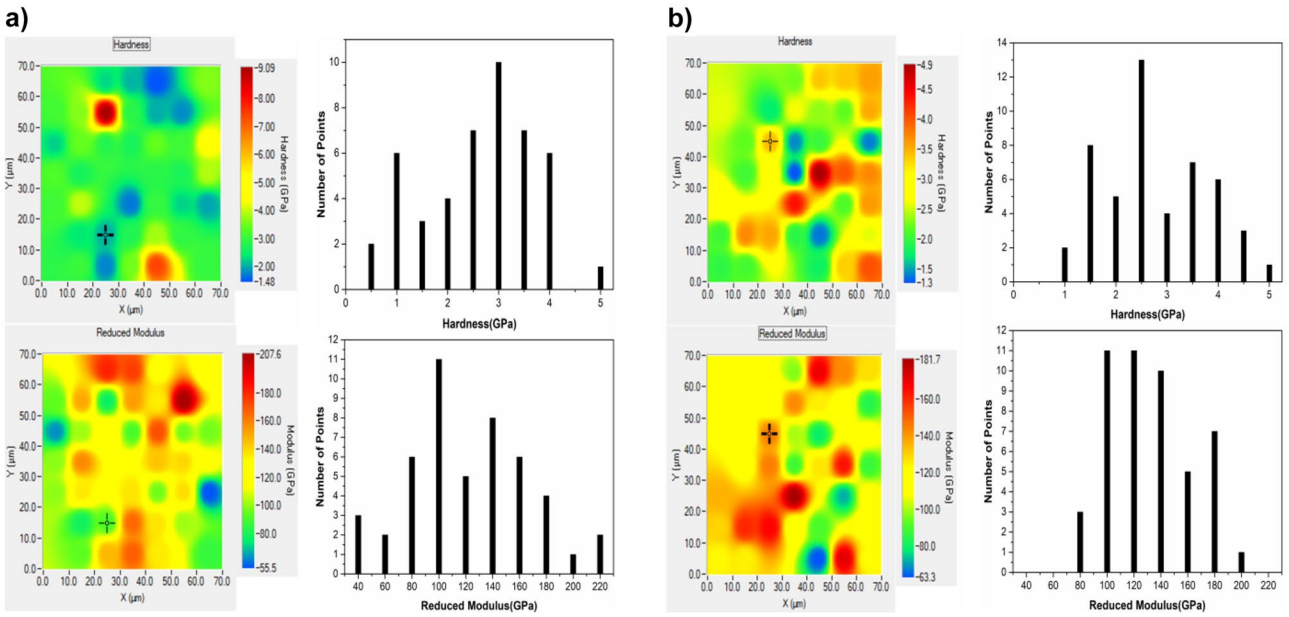


**Fig. 7** XPM plots and XPM histogram graphics of **a** P(mDOPA)-co-P(DMAEMA$^+$)/Pox(mDOPA)-Ag$^0$/PAH and **b** P(mDOPA)-*co*-P(DMAEMA$^+$)/ Pox(mDOPA)-Ag$^0$/PAH/PPIX-ED

The load-displacement curves of the tested samples which indicate the extent of penetration of the indenter within the samples demonstrated that the maximum displacement at the curves of the final P(mDOPA)-*co*-P(DMAEMA$^+$)/Pox(mDOPA)-Ag$^0$/PAH/PPIX-ED coating (Fig. 6c) was lower compared to the P(mDOPA)-co-P(DMAEMA$^+$)/Pox(mDOPA)-Ag$^0$/PAH (Fig. 6a). This is an indication of higher resistance of the final coating against the indenter movement inside the material and better nanomechanical properties. These results were supported by the nanomechanical characteristics like hardness (H) and elastic modulus (E), measured as a function of contact depth (hc). The linear decrease of H and E values with increased contact depth was observed and this can be associated with the viscoelastic properties of the coatings, which in depth lead to slower relaxation of the applied normal stress. A similar observation was reported in our previous investigation concerning the nanomechanical properties of mussels-inspired coatings on SS [14]. The calculated average values of H and E for the SS coated by P(mDOPA)-*co*-P(DMAEMA$^+$)/Pox(mDOPA)-Ag$^0$/PAH nanogel were 1.75 GPa and 96.76 GPa (Fig. 6b) relative to 1.82 GPa and 160.9 GPa for SS coated by P(mDOPA)-*co*-P(DMAEMA$^+$)/Pox(mDOPA)-Ag$^0$/PAH/PPIX-ED (Fig. 6d), which results demonstrated their high mechanical performance of the coating obtained.

**Mechanical property mapping (XPM)** Further, the P(mDOPA)-*co*-P(DMAEMA$^+$)/Pox(mDOPA)-Ag$^0$/PAH and P(mDOPA)-*co*-P(DMAEMA$^+$)/ Pox(mDOPA)-Ag$^0$ /PAH/PPIX-ED coatings were subjected to XPM analysis to get a mechanical mapping of the local surface area of the samples. The accelerated property mapping (XPM) method consists of very fast nanoindentation with high resolution by which, quantitative nanomechanical property maps and property distributions are received in a very short time compared to standard modes [30].

The mechanical property maps of the selected surface area give an evaluation of the surface homogeneity of the material. The relatively narrow histogram distribution of the nanomechanical parameters as hardness and the reduced elastic module was observed for both coatings (Fig. 7a, b), indicating a rather uniform surface hardness and elasticity.

## Antibacterial activity of photoactive polymer coatings

Finally, the antibacterial activity of the obtained photoactive coatings was demonstrated against Gram-negative *E. coli*

**Table 1** Antibacterial activity of PPIX-ED and Pox(mDOPA)-Ag$^0$/PAH nanogel

| Sample | *B. subtilis* Inhibition zone (mm) | *E. coli* Inhibition zone (mm) |
|---|---|---|
| PPIX-ED | 9.3 | 12.2 |
| Pox(mDOPA)-Ag$^0$/PAH | 9.5 | 11.2 |

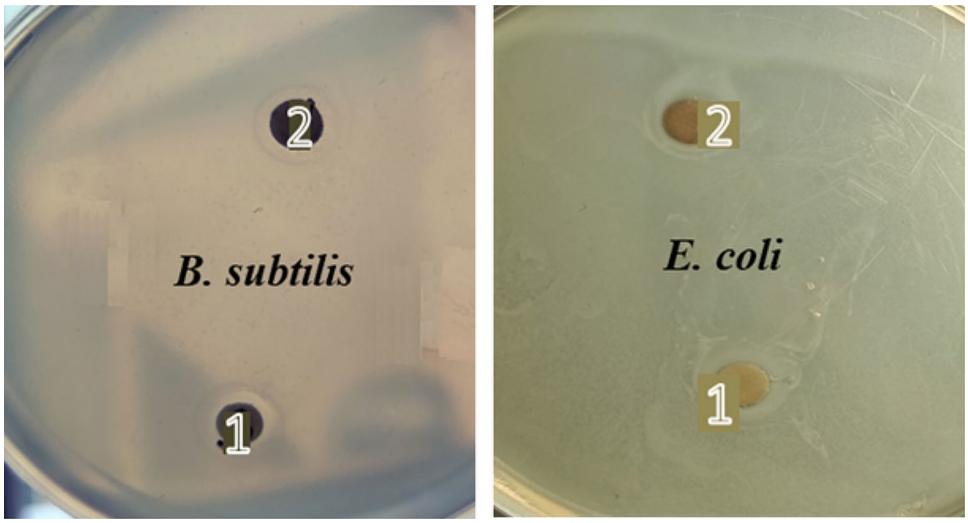


**Fig. 8** Antibacterial activity of **1** Pox(mDOPA)-$Ag^0$/PAH nanogel and **2** PPIX-ED against *B. subtilis* and *E.coli*

**Table 2** Antibacterial activity of the coatings on SS

| Sample | *B. subtilis* Inhibition zone (mm) | *E. coli* Inhibition zone (mm) |
|---|---|---|
| P(mDOPA)-*co*- P(DMAEMA$^+$) /Pox(mDOPA)/$Ag^0$/PAH | 13.1 | 15.0 |
| P(mDOPA)-*co*-P(DMAEMA$^+$) / Pox(mDOPA)-$Ag^0$/PAH/PPIX-ED | 14.0 | 17.4 |

and Gram-positive *B. subtilis* strains. Initially, the antibacterial activity of amino-modified PPIX-ED and silver loaded Pox(mDOPA)-$Ag^0$/PAH nanogel performed under light irradiation was tested using the disc diffusion method (DDM). It was found that each of the components exhibited bactericidal activity through the appearance of an inhibition zone in the range 9–12 mm (Table 1; Fig. 8). Higher bactericidal activity was observed against *E.coli* in comparison to *B. subtilis*, which was more pronounced for the discs impregnated with amino-modified PPIX-ED. The obtained results suggest that the synthesized components can be successfully used to obtain photoactive antibacterial coatings on SS.

Then, the obtained coatings deposited on SS were tested for bactericidal activity against Gram-negative *E. coli* and Gram-positive *B. subtilis* strains. For this purpose, P(mDOPA)-*co*-P(DMAEMA$^+$)/ Pox(mDOPA)-$Ag^0$/PAH deposited on a SS and a final coating of P(mDOPA)-*co*-P(DMAEMA$^+$)/ Pox(mDOPA)-$Ag^0$/PAH/PPIX-ED were examined under light irradiation using disc diffusion method (DDM). It was found that the tested samples showed antibacterial activity by the appearance of an inhibition zone in the range of 13–17 mm (Table 2; Fig. 9) in comparison to the neat SS substrate, where no inhibition zone was observed. The tested samples showed again higher antibacterial activity against G. negative *E.coli*. It is known that gram-positive and gram-negative bacteria have differences in their membrane structure, as one of the most characteristics is the thickness of the peptidoglycan layer [31]. Therefore, the higher antibacterial efficacy against *E. coli* may

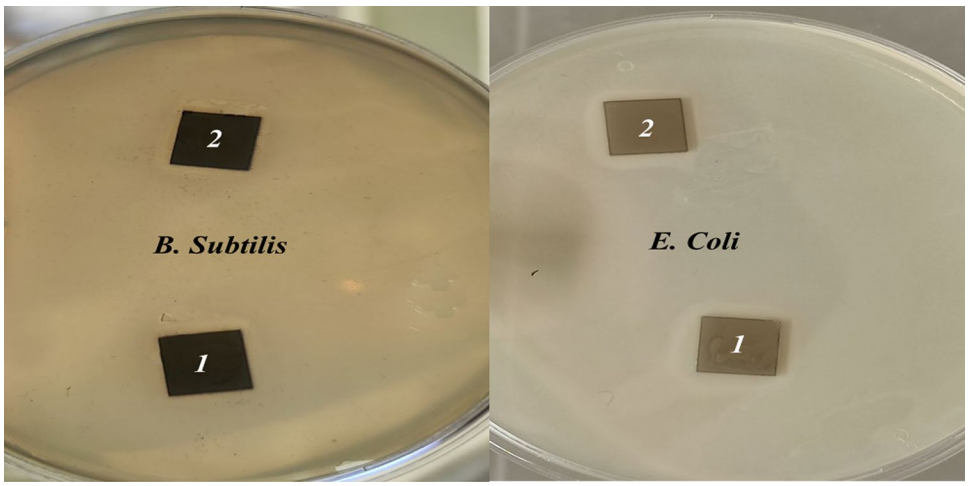


**Fig. 9** Antibacterial activity of **1** P(DMAEMA$^+$)/ Pox(mDOPA)-$Ag^0$/PAH and **2** P(mDOPA)-*co*-P(DMAEMA$^+$)/ Pox(mDOPA)-$Ag^0$/PAH/PPIX-ED against *B. subtilis* and *E.coli* by DDM

derive from the difference in their membrane structure. An increase in the antibacterial activity regardless of the strains used was observed at the final antibacterial photoactive coating, which is likely due to a combining effect of the silver nanoparticles and the photoactive PPIX-ED, which will ensure long-lasting bactericidal activity.

## Conclusions

Bio-inspired antibacterial polymer coatings with included silver nanoparticles and a porphyrin-based photosensitizer have been prepared. This was achieved using bio-inspired nanogels loaded with silver nanoparticles on stainless steel pre-coated by biomimetic glue, followed by the grafting of an amino-bearing porphyrin-based photosensitizer. SEM-EDX elemental mapping followed the deposition of the coatings and their nanomechanical properties were assessed by scratch test, nanoindentation, and XPM analyses. It was established that the deposition of the last layer based on amino-modified PPIX-ED photosensitizer significant improve as the nanomechanical properties of the coatings, as well their antibacterial activity, which was demonstrated by preliminary investigation of the antibacterial photoactivity against Gram-positive *B. subtilis* and Gram-negative *E. coli*. The results obtained showed that the photoactive antibacterial polymer coatings possess stronger antibacterial activity against the tested strains under light irradiation, in comparison to the coating, which consist only of P(DMAEMA$^+$)/Pox(mDOPA)-Ag$^0$/PAH nanogels. The results demonstrated that the obtained coatings could be used as a platform for the preparation of antibacterial polymer coatings for various applications in the medical field.

**Acknowledgements** This work was supported by the National Science Fund of Bulgaria (project no. KP-06-H29/5). Christophe Detrembleur is Research Director by F.R.S.- FNRS and thanks FNRS for funding. We acknowledge the provided access to the scientific infrastructure of the laboratory of Micro and Nanomechanics of Mechatronic Systems, with financial support by Grant No BG05M2OP001-1.002-0011-C02, financed by the Science and Education for Smart Growth Operational Program (2014–2020) and co-financed by the European Union through the European Structural and Investment funds.

**Data availability** The authors declare that the data supporting the findings of this study are available within the paper.

## Declarations

**Conflict of interest** On behalf of all authors, the corresponding author states that there is no conflict of interest.

## References

1. Sefton AM (2004) Encyclopedia of gastroenterology 740–743
2. Walker T, Canales M, Noimark S, Page K, Parkin I, Faull J, Bhatti M, Ciricet L (2017) A light-activated antimicrobial surface is active against bacterial, viral and fungal organisms. Sci Rep 7:15298
3. Noimark S, Bovis M, MacRobert AJ, Correia A, Allan E, Wilson M, Parkin IP (2013) Photobactericidal polymers; the incorporation of crystal violet and nanogold into medical grade silicone. RSC Adv 3:18383–18394
4. Page K, Wilson M, Parkin IP (2009) Antimicrobial surfaces and their potential in reducing the role of the inanimate environment in the incidence of hospital-acquired infections. J Mater Chem 19:3819–3831
5. Piccirillo C, Perni S, Gil-Thomas J, Prokopovich P, Wilson M, Pratten J, Parkin IP (2009) Antimicrobial activity of methylene blue and toluidine blue O covalently bound to a modified silicone polymer surface. J Mater Chem 19:6167–6171
6. Decraene V, Pratten J, Wilson M (2008) Novel light-activated Antimicrobial Coatings are effective against surface-deposited Staphylococcus aureus. Curr Microbiol 57:269–273
7. Naik AJT, Ismail S, Kay Ch, Wilson M, Parkin IP (2011) Antimicrobial activity of polyurethane embedded with methylene blue, toluidene blue and gold nanoparticles against Staphylococcus aureus, illuminated with white light. Mater Chem Phys 129:446–450
8. Bovis MJ, Noimark S, Woodhams JH, Kay CWM, Weiner J, Peveler WJ, Correia A, Wilson M, Allan E, Parkin IP (2015) Photosensitisation studies of silicone polymer doped with methylene blue and nanogold for antimicrobial applications. RSC Adv 5:54830–54842
9. Noimark S, Dunnill CW, Kay CWM, Perni S, Prokopovich P, Ismail S, Wilson M, Parkin IP (2012) Incorporation of methylene blue and nanogold into polyvinyl chloride catheters; a new approach for light-activated disinfection of surfaces. J Mater Chem 22:15388–15396
10. Noimark S, Allan E, Parkin IP (2014) Light-activated antimicrobial surfaces with enhanced efficacy induced by a dark-activated mechanism. Chem Sci 5:2216–2223
11. Peveler WJ, Noimark S, Azawi HA, Hwang GB, Crick CR, Allan E, Edel JB, Ivanov AP, MacRobert AJ, Parkin IP (2018) Covalently attached antimicrobial surfaces using BODIPY: improving efficiency and effectiveness. ACS Appl Mater Interfaces 10:98–104
12. Krzywiecki M, Pluczyk-Małek S, Powroznik P, Ślusarczyk C, Król-Molenda W, Smykała S, Kurek J, Koptoń P, Łapkowski M, Blacha-Grzechnik A (2021) Chemical and electronic structure characterization of electrochemically deposited nickel tetraamino-phthalocyanine: a step toward more efficient deposition techniques for organic electronics application. J Phys Chem C 125:13542–13550
13. Gusev I, Ferreira M, Versace DL, Abbad-Andaloussi S, Pluczyk-Małek S, Erfurt K, Duda A, Data P, Blacha-Grzechnik A (2022) Electrochemically deposited zinc (tetraamino)phthalocyanine as a light-activated antimicrobial coating effective against *S. Aureus*. Materials 15:975–984
14. Bryaskova R, Philipova N, Georgiev N, Lalov I, Bojinov V, Detrembleur C (2021) Photoactive mussels inspired polymer coatings: Preparation and antibacterial activity. J Appl Polym Sci 138:50769
15. Charlot A, Sciannaméa V, Lenoir S, Faure E, Jérôme R, Jérôme C, Van De Weerdt C, Martial J, Archambeau C, Willet N, Duwez AS (2009) All-in-one strategy for the fabrication of antimicrobial biomimetic films on stainless steel. Mater Chem 19:4117–4125
16. Faure E, Lecomte P, Lenoir S, Vreuls C, Van De Weerdt C, Archambeau C, Martial J, Jérôme C, Duwez AS, Detrembleur C (2011) Sustainable and bio-inspired chemistry for robust antibacterial activity of stainless steel. J Mater Chem 21:7901–7904
17. Faure E, Falentin-Daudré C, Lanero TS, Vreuls C, Zocchi G, Van De Weerdt C, Martial J, Jérôme C, Duwez AS, Detrembleur C

(2012) Functional nanogels as platforms for imparting antibacterial, antibiofilm, and antiadhesion activities to stainless steel. Adv Funct Mater 22:5271–5282
18. Faure E, Falentin-Daudré C, Jérôme C, Lyskawa J, Fournier D, Woisel P, Detrembleur C (2013) Catechols as versatile platforms in polymer chemistry. Prog Polym Sci 38:236–270
19. Patil N, Jerome C, Detrembleur C (2018) Recent advances in the synthesis of catechol-derived (bio) polymers for applications in energy storage and environment. Prog Polym Sci 82:34–91
20. Reis ER, Metze K, Nicola EMD, Nicola JH, Borissevitch IE (2013) Photodynamic activity of protoporphyrin IX in harderian glands of Wistar rats: monitoring by gland fluorescence. J Lumin 137:32–36
21. Javed F, Samaranayake LP, Romanos GE (2014) Treatment of oral fungal infections using antimicrobial photodynamic therapy: a systematic review of currently available evidence. Photochem Photobiol Sci 13:726–734
22. Bozja J, Sherrill J, Michielsen S, Stojiljkovic I (2003) Porphyrin-based, light-activated antimicrobial materials. J Polym Sci Part A: Polym Chem 41:2297–2303
23. Vasilev K (2019) Nanoengineered antibacterial coatings and materials: a perspective. Coatings 9:654–666
24. Lyutakov O, Hejna O, Solovyev A, Kalachyova Y, Svorcik V (2014) Polymethylmethacrylate doped with porphyrin and silver nanoparticles as light-activated antimicrobial material. RSC Adv 4:50624–50630
25. Philipova N, Georgiev N, Ganchev D, Lalov I, Bryaskova R (2023) Porhyrine/silver nanoparticles based photoactive antibacterial coatings. J Chem Technol Metall 58:275–282
26. Batakliev T, Ivanov E, Angelov V, Spinelli G, Kotsilkova R (2022) Advanced nanomechanical characterization of biopolymer films containing GNPs and MWCNTs in hybrid composite structure. Nanomaterials 12:709
27. Lei Z, Zhang L, Wie X (2008) One-step synthesis of silver nanoparticles by sonication or heating using amphiphilic block copolymer as templates. J Colloid Interface Sci 324:216–219
28. Jennett NM, Owen-Jones S (2002) The scratch test: calibration, verification and the use of a certified reference material, NPL Measurement Good Practice Guide No. 54
29. Ahmadabadi N, Zadeh KK, Bhaskaran M, Sriram S (2013) In situ nanoindentation: probing nanoscale multifunctionality. Prog Mater Sci 58:1–29
30. Němeček J, Lukeš J (2020) High-speed mechanical mapping of blended cement pastes and its comparison with standard ˇ modes of nanoindentation. Mater Today Commun 23:100806
31. Kim JS, Kuk E, Yu KN, Kim JH, Park SJ, Lee HJ (2007) Antimicrobial effects of silver nanoparticles. Nanomed Nanotechnol Biol Med 3:95–101